

DeepSleepNet: a Model for Automatic Sleep Stage Scoring based on Raw Single-Channel EEG

Akara Supratak, Hao Dong, Chao Wu, and Yike Guo*

Abstract—Objective: The present study proposes a deep learning model, named DeepSleepNet, for automatic sleep stage scoring based on raw single-channel EEG, and a two-step training algorithm used to effectively train such model. **Methods:** Most of the existing methods rely on hand-engineered features which require prior knowledge about sleep stage scoring. Only a few of them encode the temporal information such as stage transition rules, which is important to correctly identify the next possible sleep stages, into the extracted features. In the proposed model, we utilize Convolutional Neural Networks (CNNs) to extract time-invariant features, and bidirectional Long Short-Term Memory (bidirectional-LSTM) to learn transition rules among sleep stages from EEG epochs. We implement a two-step training algorithm that pre-trains the model with oversampled dataset to alleviate class-imbalance problems and fine-tunes the model with sequences of EEG epochs to encode the temporal information into the model. **Results:** We applied our model to the F4-EOG (Left) channel from a set of 62 subjects in an open-access database, containing 58600 EEG epochs (~488 hours). The results demonstrated that our model scored the EEG epochs with the accuracy of 86.2% and the macro F1-score of 81.7. **Conclusion:** Without utilizing any hand-engineered features, our model can achieve a similar sleep stage scoring performance with the highest macro F1-score compared to the state-of-the-art methods. **Significance:** This study proposes a deep learning model that can automatically learn features from raw single-channel EEG, and accurately score EEG epochs as good as the state-of-the-art hand-engineering methods.

Index Terms—Sleep Stage Scoring, Deep Learning, Single-channel EEG.

I. INTRODUCTION

SLEEP plays an important role in human health. Being able to monitor how well do people sleep in each day have a significant impact on medical research and practice [1].

Typically, sleep experts determine the quality of sleep using electrical activity recorded from sensors attached to different parts of the body. A set of signals from these sensors is called a polysomnogram (PSG), consisting of an electroencephalogram (EEG), an electrooculogram (EOG), an electromyogram (EMG), and an electrocardiogram (ECG). This PSG is segmented into 30-s epochs (or 20-s epochs, but the 30-s epochs is more common), which are then be classified into different sleep stages by the experts according to sleep manuals such as the Rechtschaffen and Kales (R&K) [2] and the American Academy of Sleep Medicine (AASM) [3]. This process is called sleep stage scoring or sleep stage classification. This manual approach is, however, labor-intensive

A. Supratak, H. Dong, C. Wu and Y. Guo are with the Department of Computing, Imperial College London, London, SW7 2AZ, UK (e-mail: {as12212, hao.dong11, chao.wu, y.guo}@ic.ac.uk)

*Corresponding author

and time-consuming due to the need for PSG recordings from several sensors attached to subjects over several nights.

There have been a number of studies trying to develop a method to automate sleep stage scoring based on multiple signals such as EEG, EOG and EMG [4], [5], or single-channel EEG [6]–[9]. These methods firstly extract time-domain, frequency-domain and time-frequency-domain features from each recording epoch. The features are then used to train classifiers to identify the sleep stage of the epoch. However, we believe that these methods may well not generalize to a larger population due to the heterogeneity among subjects and recording hardware. This is because these features were hand-engineered based on the characteristics of the available dataset.

Recently, deep learning, a branch of machine learning that utilizes multiple layers of linear and non-linear processing units to learn hierarchical representations or features from input data, has been employed in sleep stage scoring. For instance, the authors in [10] have investigated a capability of Deep Belief Nets (DBNs) to learn probabilistic representations from preprocessed raw PSG. Convolutional Neural Networks (CNNs) have also been applied to learn multiple filters that are used to convolve with small portions of input data (i.e., convolution) to extract time-invariant features from raw Fpz-Cz EEG channel [11]. However, the results from the literature showed that applying deep learning on hand-engineered features performed better than on raw signals [6], [10]. This might well be because the authors did not consider temporal information that sleep experts use when they determine the sleep stage of each epoch.

Only a few number of literature have explored Recurrent Neural Networks (RNNs) in sleep stage scoring. RNNs are capable of conditioning outputs on all previous inputs, as they maintain internal memory and utilizes feedback (or loop) connections to learn temporal information from sequences of inputs. The main advantage of RNNs is that they can be trained to learn long-term dependencies or transition rules [3] that sleep experts use to identify the next possible sleep stages from a sequence of PSG epochs. Elman RNNs have been applied on energy features from the Fpz-Cz EEG channel [12]. In our previous work [13], we also applied Long Short-Term Memory (LSTM) on time-frequency-domain features from the F4-EOG and Fp2-EOG channels separately. Even though the reported results were promising, these methods still rely on hand-engineered features.

This paper introduces *DeepSleepNet*, a model for automatic sleep stage scoring based on raw single-channel EEG, which is different from the existing works that develop algorithms to extract features from EEG. We aim to automate the process

of hand-engineering features by utilizing the feature extraction capabilities of deep learning. The main contributions of this work are as follows:

- We develop a new model architecture that utilizes two CNNs with different filter sizes at the first layers and bidirectional-LSTMs. The CNNs can be trained to learn filters to extract time-invariant features from raw single-channel EEG, while the bidirectional-LSTMs can be trained to encode temporal information such as sleep stage transition rules into the model.
- We implement a two-step training algorithm that can effectively train our model end-to-end via backpropagation, while preventing the model from suffering class imbalance problem (i.e., learning to classify only the majority of sleep stages) presented in a large sleep dataset.
- We show that our model can be trained to automatically learn features directly from raw single-channel EEGs, and can achieve a similar sleep stage scoring performance, and the best macro-F1 score compared to the state-of-the-art methods without utilizing any hand-engineered features.

We believe that our approach provides a general framework for classifying sleep stages based on a single-channel EEG from wearable devices, and potentially for other multi-class classification problems that rely on single-channel biosignals such as EEG and ECG.

II. DEEPSLEEPNET

The architecture of DeepSleepNet is shown in Fig. 1. It can be seen that our model consists of two main parts. The first part is representation learning, which can be trained to learn filters to extract time-invariant features from each of raw single-channel EEG epochs. The second part is sequence residual learning, which can be trained to encode the temporal information such as stage transition rules [3] from a sequence of EEG epochs.

A. Representation Learning

We employ two CNNs with small and large filter sizes at the first layers to extract time-invariant features from raw single-channel 30-s EEG epochs. This architecture is inspired by the way signal processing experts control the trade-off between temporal and frequency precision in their feature extraction algorithms [14]. The small filter is better to capture temporal information (i.e., when certain of EEG patterns appear), while the larger filter is better to capture frequency information (i.e., frequency components).

In our model, each CNN consists of four convolutional layers and two max-pooling layers. Each convolutional layer performs three operations sequentially: 1D-convolution with its filters, batch normalization [15], and applying the rectified linear unit (ReLU) activation (i.e., $relu(x) = \max(0, x)$). Each pooling layer downsamples inputs using *max* operation. The specifications of the filter sizes, the number of filters, stride sizes and pooling sizes can be found in Fig. 1. Each *conv* block shows a filter size, the number of filters, and a stride

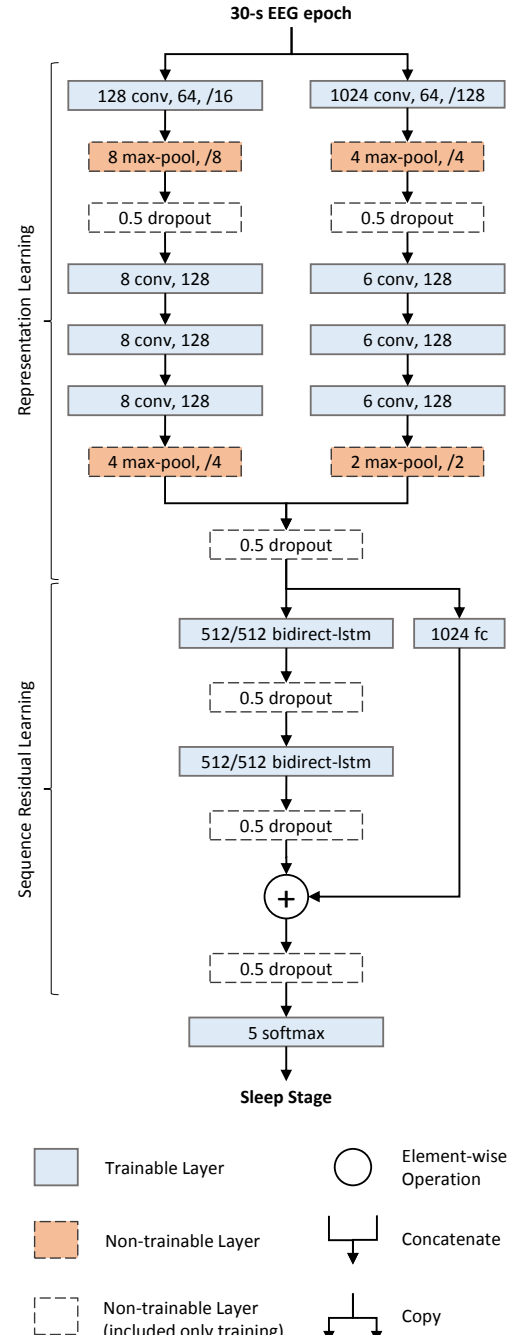


Fig. 1. An overview architecture of DeepSleepNet consisting of two main parts: representation learning and sequence residual learning. Each trainable layer is a layer containing parameters to be optimized during a training process.

size. Each *max-pool* block shows a pooling size and a stride size. We will explain *dropout* blocks later in Section III-C.

Formally, suppose there are N 30-s EEG epochs $\{\mathbf{x}_1, \dots, \mathbf{x}_N\}$ from single-channel EEG. We use the two CNNs to extract the i -th feature \mathbf{a}_i from the i -th EEG epoch \mathbf{x}_i as follows:

$$\mathbf{h}_i^s = CNN_{\theta_s}(\mathbf{x}_i) \quad (1)$$

$$\mathbf{h}_i^l = CNN_{\theta_l}(\mathbf{x}_i) \quad (2)$$

$$\mathbf{a}_i = \mathbf{h}_i^s \parallel \mathbf{h}_i^l \quad (3)$$

where $CNN(x_i)$ is a function that transform a 30-s EEG epoch \mathbf{x}_i into a feature vector \mathbf{h}_i using a CNN, θ_s and θ_l are parameters of the CNNs with small and large filter sizes in the first layer respectively, and $||$ is a concatenate operation that combines the outputs from two CNNs together. These concatenated or linked features $\{\mathbf{a}_1, \dots, \mathbf{a}_N\}$ are then forwarded to the sequence residual learning part.

B. Sequence Residual Learning

We apply the residual learning framework [16] to design our sequence residual learning part. This part consists of two main components: bidirectional-LSTMs [17] and a shortcut connection (see Fig. 1).

We employ two layers of bidirectional-LSTMs to learn temporal information such as stage transition rules [3] which sleep experts use to determine the next possible sleep stages based on the previous stages. For instance, the AASM manual suggests that if a subject is in sleep stage N2, continue to score epochs with low amplitude and mixed frequency EEG activity as N2 even though K complexes or sleep spindles are not present. In this case, the bidirectional-LSTMs can learn to remember that it has seen the stage N2, and continue to score successive epochs as N2 if they still detect the low amplitude and mixed frequency EEG activity. Bidirectional-LSTMs extends the LSTM [18] by having two LSTMs process forward and backward input sequences independently [17]. In other words, the outputs from forward and backward LSTMs are not connected to each other. The model is therefore able to exploit information both from the past and the future. We also use peephole connections [19], [20] in our LSTMs which allow their gating mechanism to inspect their current memory cell before the modification.

We use a shortcut connect to reformulate the computation of this part into a residual function. This enables our model to be able to add temporal information it learns from the previous input sequences into the feature extracted from the CNNs. We also use a fully-connected layer in the shortcut connection to transform the features from the CNNs into a vector that can be added to the output from the LSTMs. This layer performs matrix multiplication with its weight parameters, batch normalization, and applying the ReLU activation sequentially.

Formally, suppose there are N features from the CNNs $\{\mathbf{a}_1, \dots, \mathbf{a}_N\}$ arranged sequentially and $t = 1 \dots N$ denotes the time index of 30-s EEG epochs, our sequence residual learning is defined as follows:

$$\mathbf{h}_t^f, \mathbf{c}_t^f = LSTM_{\theta_f}(\mathbf{h}_{t-1}^f, \mathbf{c}_{t-1}^f, \mathbf{a}_t) \quad (4)$$

$$\mathbf{h}_t^b, \mathbf{c}_t^b = LSTM_{\theta_b}(\mathbf{h}_{t+1}^b, \mathbf{c}_{t+1}^b, \mathbf{a}_t) \quad (5)$$

$$\mathbf{o}_t = \mathbf{h}_t^f || \mathbf{h}_t^b + FC_{\theta}(\mathbf{a}_t) \quad (6)$$

where $LSTM$ represents a function that processes sequences of features \mathbf{a}_t using the two-layers LSTM parameterized by θ_f and θ_b for forward and backward directions; \mathbf{h} and \mathbf{c} are vectors of hidden and cell states of the LSTMs; $\mathbf{h}_0^f, \mathbf{c}_0^f, \mathbf{h}_{N+1}^b$ and \mathbf{c}_{N+1}^b of forward and backward LSTMs are set to zero vectors; FC represents a function that transform features \mathbf{a}_t into a vector that can be added (element-wise) with the concatenated output vector $\mathbf{h}_t^f || \mathbf{h}_t^b$ from the bidirectional-LSTMs.

The specifications of the hidden size of forward and backward LSTMs, and the fully-connected layers can be found in Fig. 1. Each *bidirect-lstm* block shows hidden sizes of forward and backward LSTMs. Each *fc* block shows a hidden size.

It should be noted that the hidden and cell states $\mathbf{h}_t^f, \mathbf{h}_t^b, \mathbf{c}_t^f$ and \mathbf{c}_t^b in (4) and (5) will be re-initialized to zeros at the beginning of each patient data during the training and testing. This is to make sure that the model uses only temporal information from the current subject data for both training and testing.

C. Model Specification

Table I shows the model specification for DeepSleepNet. This specification is designed for single-channel EEG with a sampling rate of 256 Hz.

For the representation learning part, the parameters of the CNN-1 and CNN-2 were selected with the aim to capture temporal and frequency information from the EEG according to the guideline provided by [14]. For instance, the filter size of the *conv1* layers of the CNN-1 was set to 128 (half of the sampling rate), and its stride size was set to 16 to detect when certain of EEG patterns appear. On the other hand, the filter size of the *conv1* layer of the CNN-2 was set to 1024 (four times of the sampling rate) to better capture the frequency components from the EEG. Its stride size was also set to 128, which is higher than the *conv1* layer of the CNN-1, as it is not necessary to perform a fine-grained convolution to extract frequency components. The filter and stride sizes of the subsequent convolutional layers *conv2_1-3* were chosen to be small fix sizes. It is believed that the use of multiple convolutional layers with a small filter size instead of a single convolutional layer with a large filter can reduce the number of parameters and the computational cost, and can still achieve the similar level of model expressiveness [21].

For the sequence residual learning part, the parameters of the *bidirect-lstm* and *fc* layers were set to 1024, which was approximately three times smaller than the concatenation output size, to restrict our model to select and combine only the important features from the representation learning part. This is to prevent our model from overfitting.

The model specification might vary depending on the characteristics of EEG and/or the recording devices. For instance, the EEG data with a sampling rate of 200 Hz might have filter sizes of 100 and 800 for the *conv1* layer of the CNN-1 and CNN-2 respectively. We believe that our basic structure and the workflow of the representation learning and sequence residual learning parts can be generalized to different EEG characteristics such as the ones recorded with different hardware and software).

III. TWO-STEP TRAINING ALGORITHM

The two-step training algorithm (see Algorithm 1) is a technique we develop to effectively train our model end-to-end via backpropagation, while preventing the model from suffering class imbalance problem (i.e., learning to classify only the majority of sleep stages) present in a large sleep dataset. The algorithm first pre-trains the representation learning part of the

TABLE I
MODEL SPECIFICATION FOR DEEPSLEEPNET

Part I: Representation Learning						
Layer name	CNN-1		CNN-2			
	Output size	Specification	Output size	Specification		
conv1	480x64	filter size: 128 # of filters: 64 stride size: 16	60x64	filter size: 1024 # of filters: 64 stride size: 128		
max-pool1	60x64	pool size: 8 stride size: 8	15x64	pool size: 4 stride size: 4		
conv2_[1-3]*	60x128	filter size: 8 # of filters: 128 stride size: 1	15x128	filter size: 6 # of filters: 128 stride size: 1		
max-pool2	15x128	pool size: 4 stride size: 4	8x128	pool size: 2 stride size: 2		
	flatten into a vector output size: 1920		flatten input a vector output size: 1024			
	concatenate two vectors into a single vector output size: 2944					
Part II: Sequence Residual Learning						
Layer name	Output size		Specification			
bidirect-lstm_[1-2]*	1024		forward hidden size: 512 backward hidden size: 512			
fc	1024		hidden size: 1024			
	add outputs from bi-lstm and fc layers (i.e., shortcut connection) output size: 1024					
softmax	5		hidden size: 5			

*a stack of layers that have the same output size and specification

model and then fine-tunes the whole model using two different learning rates. We use the cross-entropy loss to quantify the agreement between the predicted and the target sleep stages in both of these training steps.

A. Pre-training

The first step is to perform a supervised pre-training on the representation learning part of the model with a class-balance training set so that the model does not overfit to the majority of sleep stages. This can be seen in Algorithm 1, lines 1-8. Specifically, the two CNNs are extracted from the model and then stacked with a softmax layer *softmax*. It is important to note that this is a different softmax layer from the one in the model. This stacked softmax layer is only used in this step to pre-train the two CNNs, in which its parameters are discarded at the end of the pre-training. We denote these two CNNs stacked with *softmax* as *pre_model*. Then the *pre_model* is trained with a class-balance training set using a mini-batch gradient-based optimizer called Adam [22] with a learning rate, *lr*. At the end of the pre-training, the softmax layer is discarded. The class-balance training set is obtained from duplicating the minority sleep stages in the original training set such that all sleep stage have the same number of samples (i.e., oversampling).

B. Fine-tuning

The second step is to perform a supervised fine-tuning on the whole model with a sequential training set. This can be

seen in Algorithm 1, lines 9-19. This step is to encode the stage transition rules into the model as well as to perform necessary adjustments on the pre-trained CNNs. Specifically, the parameters θ_s and θ_l of the two CNNs of *model* are replaced with the ones from the *pre_model*. Then the *model* is trained with the sequence training set using a mini-batch Adam optimizer with two different learning rates, *lr*₁ and *lr*₂. As the CNNs part has already been pre-trained, we, therefore, use a lower learning rate *lr*₁ for the CNNs part and a higher learning rate *lr*₂ for the sequence residual learning part, and a softmax layer. We found that when we used the same learning rate to fine-tune the whole network, the pre-trained CNN parameters were excessively adjusted to the sequential data, which were not class-balanced. As a consequence, the model started to overfit to the majority of the sleep stages toward the end of the fine-tuning. Therefore, two different learning rates are used during fine-tuning. Also, we use a heuristic gradient clipping technique to prevent the exploding gradients, which is a well-known problem when training RNNs such as LSTMs [23]. This technique rescales the gradients to smaller values using their global norm whenever they exceed a pre-defined threshold. The sequential training set is obtained by arranging the original training set sequentially according to time across all subjects.

C. Regularization

We employed two regularization techniques to help prevent overfitting problems. The first technique was dropout [24], [25]

Algorithm 1 Two-step Training**Input:** *model, data***Output:** *model**Initialization:*

```

1:  $CNN_{\theta_s, \theta_l} \leftarrow copy\_cnns(model)$ 
2:  $pre\_model = stack(CNN_{\theta_s, \theta_l}, softmax)$ 
3:  $data_{over} = oversample(data)$ 

```

Pre-training Step:

```

4: for  $i = 1$  to  $n\_pretrain\_epochs$  do
5:   for each batch in shuffle(dataover) do
6:      $pre\_model \leftarrow adam_{lr}(pre\_model, batch)$ 
7:   end for
8: end for
9: Fine-tuning Step:
10:  $\theta_s, \theta_l \leftarrow get\_cnn\_params(pre\_model)$ 
11:  $model \leftarrow set\_params(model, (\theta_s, \theta_l))$ 
12: for  $i = 1$  to  $n\_finetune\_epochs$  do
13:   for each subject in data do
14:      $model \leftarrow reset\_lstm\_cell\_state(model)$ 
15:      $subject\_data_{seq} \leftarrow arrange(subject)$ 
16:     for each batch in subject_dataseq do
17:        $model \leftarrow adam_{lr_1, lr_2}(model, batch)$ 
18:     end for
19:   end for
20: end for
return model

```

IV. RESULTS**A. Data**

We evaluated our model with an open-access database of polysomnographic biosignals, named Montreal Archive of Sleep Studies (MASS) [26]. There were five subsets of recordings, SS1-SS5, which were organized according to their research and acquisition protocols. We used data from SS3, which contained PSG recordings from 62 subjects (age 42.5 ± 18.9). Each recording contained 20 scalp-EEG, 2 EOG (left and right), 3 EMG and 1 ECG channels. The EEG electrodes were positioned according to the international 10-20 system, and the EOG electrodes were positioned diagonally on the outer edges of the eyes. EEG and EOG recordings were preprocessed with a notch filter of 60 Hz, and band-pass filters of 0.30-100 Hz (EEG) and 0.10-100 Hz (EOG). All EEG and EOG recordings had the same sampling rate of 256 Hz. These recordings were manually classified into one of the five sleep stages, W, N1, N2, N3, and REM, by a sleep expert according to the AASM standard [3]. There were also movement artifacts at the beginning and the end of each subject's recordings that were labeled as UNKNOWN.

We evaluated our model using the F4-EOG (Left) channel, which was obtained via montage reformatting [27] without any further pre-processing. We excluded the UNKNOWN stages from the dataset, which resulted in 58600 of 30-s EEG epochs (or around 488 hours) in total.

that randomly sets the input values to 0 (i.e., dropping units along with their connection) with the specified probability during training. Dropout layers with the probability of 0.5 were used throughout the model as shown in Fig. 1. In our experiment, we found that inserting dropout layers after the convolution layers slowed down the convergence of our training process without performance gains. Therefore, we only used dropout after the pooling layers in the representation learning part. In the sequence learning part, on the other hand, the locations of the dropout layers did not affect classification performance much. Thus we used dropout after each layer in this part. It is important to note that these dropout layers were used for training only, and were removed from the model during testing to provide deterministic outputs.

The second technique was L2 weight decay, which adds a penalty term into a loss function to prevent large values of the parameters in the model (i.e., exploding gradients). We only applied the weight decay on the first layers of the two CNNs because of the two main reasons. Firstly, it is pointed out in [23] that L2 weight decay can limit the model capabilities of learning long-term dependencies. Secondly, we found that, without the weight decay, the filters of the first layers in the CNNs overfitted to noises or artifacts in EEG data. This weight decay helped the model learn smoother filters (i.e., containing less high-frequency elements) which resulted in slightly performance gains. In our experiment, the weight decay parameter that defines the degree of penalty, lambda, was set to 10^{-3} .

B. Experimental Design

We evaluated our model using a 31-fold cross-validation scheme. Specifically, in each fold, we used recordings from 60 subjects to train the model, and from the remaining 2 subjects to test the trained model. This process was repeated 31 times so that all of the recordings were tested. Then we combined the predicted sleep stages from all folds, and computed the performance metrics, which will be discussed in Section IV-C.

C. Performance Metrics

We evaluated the performance of our model using per-class precision (PR), per-class recall (RE), per-class F1-score (F1), macro-averaging F1-score (MF1), and overall accuracy (ACC) [28]. The per-class metrics are computed by considering a single class as a positive class, and all other classes combined as a negative class. The MF1 and ACC are calculated as follows:

$$ACC = \frac{\sum_{c=1}^C TP_c}{N} \quad (7)$$

$$MF1 = \frac{\sum_{c=1}^C F1_c}{C} \quad (8)$$

where TP_c is the true positives of class c , $F1_c$ is per-class F1-score of class c , C is the number of sleep stages, and N is the total number of test epochs.

D. Training Parameters

The representation learning part was pre-trained using the oversampled training set with the mini-batch size of 100. The Adam optimizer's parameters lr , $beta1$, and $beta2$ were set to 0.0001, 0.9 and 0.999 respectively. Then the whole model was fine-tuned using the sequential training set. Specifically, we equally split the sequences of 30-s EEG epochs from each subject data into 10 sub-sequences (i.e., batch size was 10). Then we fed 25 epochs (i.e., sequence length was 25) from each sub-sequence yielding 250 epochs per one step training. The Adam optimizer's parameters were similar to the pre-training step except that the learning rate of each part of the model, $lr1$ and $lr2$, were set to 10^{-6} and 10^{-4} respectively. The threshold of the gradient clipping was set to 10. With this setting, we found that the pre-training and fine-tuning steps started to converge after 100 and 200 training epochs respectively.

It should be noted that we used the default value for the most of the parameters such as $beta1$, $beta2$ and the threshold of the gradient clipping, which can be found in the literature. We only experimented with the mini-batch size (from 50 to 200) during the pre-training, the batch size (from 5 to 40) and sequence length (from 5 to 40) during fine-tuning, and the learning rates (from 10^{-3} to 10^{-6}).

For the batch normalization in *conv* and *fc* blocks, the ϵ constant of 10^{-5} was added to the mini-batch variance for numerical stability. The mean and variance of the training set, which were used as fixed parameters during testing, were estimated by computing the moving average of with a decay rate of 0.999 from the sampling mean and variance of each mini-batch.

E. Implementation

We implemented our model using TensorLayer (<https://github.com/zsdonghao/tensorlayer>), which is a deep learning library extended from Google Tensorflow [29]. This library allows us to deploy numerical computation such as the training and validation tasks to multiple CPUs and GPUs. We ran the 31-fold cross-validation using the eTRIKS Analytical Environment (eAE) (<https://eae.doc.ic.ac.uk/>), which provides a cluster of high-performance computing nodes. Each node was equipped with an NVIDIA GeForce GTX 980. The training time for each validation fold was approximately 3 hours on each node. The testing or prediction time for each batch of 25 EEG epochs (according to the sequence length specified during training in Section IV-D) was approximately 50 milliseconds on each node.

F. Sleep Stage Scoring Performance

Table II shows a confusion matrix obtained from 31-fold cross-validation on the F4-EOG (Left) channel using our DeepSleepNet model. Each row and column represent the number of 30-s EEG epochs of each sleep stage classified by the sleep expert and our model respectively. The numbers in bold indicate the number of epochs that were correctly classified by our model. The last three columns in each row

TABLE II
CONFUSION MATRIX OBTAINED FROM 31-FOLD CROSS-VALIDATION ON THE F4-EOG (LEFT) CHANNEL USING DEEPSLEEPNET

	Predicted					Per-class Metrics		
	W	N1	N2	N3	REM	PR	RE	F1
W	5433	572	107	13	102	87.3	87.2	87.3
N1	452	2802	827	4	639	60.4	59.3	59.8
N2	185	906	26786	1158	499	89.9	90.7	90.3
N3	18	4	1552	6077	0	83.8	79.4	81.5
REM	132	356	533	1	9442	88.4	90.2	89.3

indicate per-class performance metrics computed from the confusion matrix.

It can be seen that the poorest performance was noted for the stage N1, with the F1 of 59.8, while the F1 for other stages were significantly better, with the range between 81.5 and 90.3. Most of the misclassified stages were between N2 and N3. It can also be seen that the confusion matrix is almost symmetric via the diagonal line. This indicates that the misclassifications were less likely to be due to the imbalance-class problem.

G. Comparison with State-of-the-Art Approaches

Table III shows a comparison between our method and other sleep stage scoring methods (including our previous work [13]) that utilize hand-engineering features across ACC, MF1 and F1. The numbers in bold indicate the highest performance metrics of all methods. It can be seen that our method outperformed the state-of-the-art ones on MF1. This indicates that our method did not achieve the high overall accuracy because it favored the majority of the sleep stages than the minority ones. Even though our method did not give the highest overall accuracy, it is important to emphasize that we evaluated our method on a much larger sleep dataset (i.e., 58600 of 30-s epochs or around 488 hours) compared to [8] and [12]. Moreover, without sacrifice the scoring performance on the other stages, our approach also gave the highest per-class F1-score on the stage N1, which is the most difficult sleep stage to classify.

H. Sequence Residual Learning

Table IV shows a confusion matrix obtained from 31-fold cross-validation on the F4-EOG (Left) channel using DeepSleepNet without the sequence residual learning part (i.e., using the *pre_model* in Algorithm 1). It can be seen that the F1 of all sleep stages, except the stage N3, were lower than the ones in Table II. This was because of an increase in the misclassifications between the pairs of N1-N2, N2-N3 and N1-REM. This may well be due to the effects of oversampling the training set to have balanced-class samples. As a consequence the model tended to predict more of stages N1 and N3. These results indicated that the process to stack the pre-trained representation learning part with the sequence residual learning part, and then fine-tune the both parts with sequential training set helped improve the classification performance.

TABLE III

COMPARISON BETWEEN DEEPSLEEPNET AND OTHER SLEEP STAGE SCORING METHODS THAT UTILIZES HAND-ENGINEERING FEATURES ACROSS OVERALL ACCURACY (ACC), MACRO-F1 SCORE (MF1), AND PER-CLASS F1-SCORE (F1)

Methods	EEG Channel	Test Epochs	Overall Metrics		Per-class F1-Score (F1)				
			ACC	MF1	W	N1	N2	N3	REM
Liang <i>et al.</i> (2012) [8]	C3-A2	8480	88.1	75.4	77.5	31.0	90.1	86.0	91.5
Fraiwan <i>et al.</i> (2012) [7]	C3-A1	6891	82.6	74.7	91.5	47.6	82.6	74.2	77.8
Hsu <i>et al.</i> (2013) [12]	Fpz-Cz	960	90.3	76.5	77.3	46.5	94.9	72.2	91.8
Tsinalis <i>et al.</i> (2016) [6]	Fpz-Cz	37022	78.9	73.7	71.6	47.0	84.6	84.0	81.4
Dong <i>et al.</i> (2016) [13]	F4-EOG (Left)	59066	85.9	80.5	84.6	56.3	90.7	84.8	86.1
DeepSleepNet (current)	F4-EOG (Left)	58600	86.2	81.7	87.3	59.8	90.3	81.5	89.3

I. Model Analysis

To better understanding how our model classified a sequence of 30-s EEG epochs, we analyzed and compared: 1) the learned filters at the first convolutional layers of the two CNNs in the representation learning part; and 2) the memory cells inside the bidirectional-LSTMs in the sequence residual learning part across 31 cross-validation folds.

Firstly, we analyzed how our model utilized the learned filter at the first convolutional layers of the two CNNs to classify different sleep stages. Specifically, we determined which filters were mostly active for each sleep stage by computing the average of the sum of the activations of all filters across samples of each sleep stage. Formally, suppose there were N 30-s EEG epochs from each validation fold $\{\mathbf{x}_1, \dots, \mathbf{x}_N\}$. We fed these epochs to our model to obtain activations \mathbf{z} from the first convolutional layer of each CNN: $\{\mathbf{z}_1, \dots, \mathbf{z}_N\}$, where $\mathbf{z}_i \in \mathbb{R}^{p \times q}$, and p and q are the activation output size and the number of filters of the first convolutional layer. The average of the sum of the activations of the filter k for the sleep stage c is computed as follows:

$$u_{c,k} = \frac{\sum_{i=1}^{N_{y_{pred}=c}} \sum_{j=1}^q z_{i,j,k}}{N_{y_{pred}=c}} \quad (9)$$

where $u_{c,k}$ is the average of the sum of the activation of the filter k for sleep stage c , $z_{i,j,k}$ is the j -th index of the activation vector \mathbf{z}_i of the filter k , and $N_{y_{pred}=c}$ is the number of EEG epochs that our model predicted as stage c . After we computed the $u_{c,k}$ of all filters for sleep stage c , we rescaled them into a range of 0 and 1. We denote this scaled k -dimension vector \mathbf{u}_c as *filter activations* for stage c . This process was repeated for all sleep stages. Once we got the filter activations from all sleep stages, we stacked them together, and rearranged the order of the filters such that the filters that were mostly active for each sleep stage were grouped together. Fig. 2 illustrates an example of the filter activations from the small (a) and large (b) filters obtained by feeding our model with data from 3 subjects. Each image has 5 rows and 64 columns, corresponding to 5 sleep stages and 64 filters respectively. Each pixel represents the value of $u_{c,k}$ from (9) scaled into a range of 0 and 1, where 1 (i.e., active) is white and 0 (i.e., inactive) is black. Each row corresponds to the 64-dimension vector (i.e., k is 64) for each sleep stage c . The first row is from stage W and the last row is from stage REM. Each image also has labels indicating which filters are mostly active for

TABLE IV
CONFUSION MATRIX OBTAINED FROM 31-FOLD CROSS-VALIDATION ON THE F4-EOG (LEFT) CHANNEL USING DEEPSLEEPNET WITHOUT SEQUENCE RESIDUAL LEARNING

	Predicted					Per-class Metrics		
	W	N1	N2	N3	REM	PR	RE	F1
W	5215	709	94	19	190	84.5	83.7	84.1
N1	468	2582	747	11	916	40.8	54.7	46.8
N2	241	1846	24140	2435	872	93.4	81.7	87.2
N3	19	3	472	7156	1	74.3	93.5	82.8
REM	227	1181	383	5	8668	81.4	82.8	82.1

which sleep stages. We found that there were two types of filters: ones that were mostly active for each sleep stage, and the other ones that were mostly active for multiple sleep stages. For instance, some of the small and large filters were mostly active for both stage N2 and N3. After we had analyzed all of the filter activations from different cross-validation folds, we found that the number of active filters for different sleep stages varied across subjects, and most of the small filters were mostly active for stage N2 and N3. We also found that, for a few subjects, no small filter was active for stage N1. This might well be because there were only a few stage N1 in the dataset.

Secondly, we analyzed how our model utilized the bidirectional-LSTMs to learn the temporal information from a sequence of EEG epochs. Specifically, we investigated how the bidirectional-LSTMs managed their memory cells (i.e., c in (4) and (5)) using the visualization technique from [30]. We found several memory cells of the forward LSTMs that were interpretable. For instance, several cells were keeping track of the wakefulness or the sleep onset, which reset their values to positive numbers (i.e., active) when a subject was in the stage W or N1 respectively. The cell values then decreased to negative values (i.e., becoming inactive) during stages N2, N3 and REM (or R in short). Fig. 3 illustrates the changes of this cell value according to a sequence of sleep stages predicted by our model. The sleep stages are arranged according through time from left-to-right, and top-to-bottom. Each sleep stage color corresponds to $\tanh(c)$, where +1 (i.e., active) is blue and -1 is red (i.e., inactive). There were also other interpretable cells such as the ones that started with a high value at the beginning of each subject data and then slowly decreased with each sleep stage until the end of the subject data, or the ones

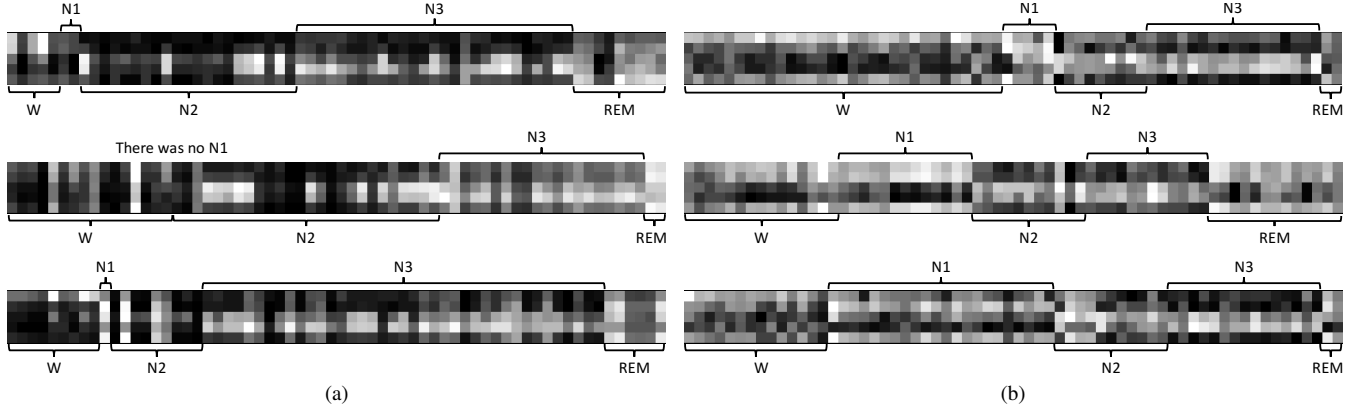


Fig. 2. Examples of the filter activations from the first convolutional layers of the two CNNs obtained by feeding our model with data from 3 subjects. The filter activations from the small filters are on the left (a), and the larger filters are on the right (b). Each image has 5 rows and 64 columns, corresponding to 5 sleep stages and 64 filters respectively. Each pixel represents the scaled value of $u_{c,k}$ from (9), where 1 (i.e., active) is white and 0 (i.e., inactive) is black. Each row corresponds to the 64-dimension vector (i.e., k is 64) for each sleep stage c . The first row is from stage W and the last row is from stage REM. Each image also has labels indicating which filters are mostly active for which sleep stages.

that turned on when they found a continuous sequence of stages N3 and REM. The existence of these cells showed that the LSTMs inside the sequence residual learning part learned to keep track of the current status of each subject, which is important to correctly identify the next sleep stages according to the stage transition rules [3].

V. DISCUSSION

To the best of our knowledge, DeepSleepNet is the first model that fully utilizes the capabilities of deep learning to automatically extract useful features from raw single-channel EEG. This is different from the existing works (including our previous work) as we did not use any hand-engineered features. The results demonstrated that our model achieved a similar performance with the highest macro F1-score, and the highest per-class F1-score on the stage N1 compared to the state-of-the-art methods. The results also showed that the temporal information learned from the sequence residual learning part helped improve the classification performance.

Our model was evaluated using the F4-EOG (Left) channel, which is from the electrodes positioned on the human face. This is different from most of the existing methods reported in the literature that rely on the electrodes at the central lobe such as Cz, C4 and C3. Our choice of EEG channel can be much easier and more comfortable to collect data either at sleep clinics or from home environment compared to the existing methods. This is because both of the electrodes do not have problems of reading the electrical activity from the hairy scalp. Even though the F4-EOG (Left) channel does not have information from the central lobe as recommended in the AASM manual [3], our results showed that our model was still able to achieve a similar performance compared to the state-of-the-art methods. As we evaluated our model on the different channel from most of the existing approaches, the performance of the per-class F1-score on stage N1 may well be improved because of the choice of the EEG channel and/or the capabilities of our model.

Fig. 3. An example of the LSTM cell that is active at the beginning of wakefulness (i.e., stage W) or the sleep onset (i.e., stage N1). The sequences of sleep stages are the predictions from DeepSleepNet on one subject data, arranged through time from left-to-right and top-to-bottom. The background color of each stage corresponds to $\tanh(c)$, where +1 is blue and -1 is red.

Based on the results of our simple model analysis, we found that our model learned several interesting features that were consistent with the AASM manual (which is the same manual the experts followed to score the MASS dataset). In the representation learning part, some of the learned filters at the first convolutional layers of the two CNNs were mostly active for stage N2-N3 and W-N1-REM (see Fig 2). This implies that our model recognized some patterns that are similar among such stages. Our model might learn the filters to detect sleep spindles that can appear in both N2 and N3 stages, and to detect different features of the eye movements from the EOG (Left) that can be used to distinguish among W, N1 and REM stages. Also, in the sequence residual learning part, we found some interpretable memory cells in the bidirectional-LSTMs such as the cells that were keeping track of the wakefulness or the sleep onset, the cells that increased or decreased its value over time, and the cells that detected a train of stage N3

and REM. Our model utilized a combination of these cells to understand the current status of each subject. For instance, our model might remember that the subject was now awake or in the stage W. The next possible stage was very likely to be either stage W or N1. It should be emphasized that our model can learn these features from raw single-channel EEG without utilizing any hand-engineered features. Moreover, we observed that the features that our model learned were consistent across different folds. Therefore, we believe that DeepSleepNet is a better approach to implement sleep stage scoring system compared to the hand-engineering ones that require prior knowledge to design feature extraction algorithms.

Even though our results are encouraging, our model is still subject to several limitations. Firstly, our model requires being trained with a sufficient amount of sleep dataset. This is due to the nature of the deep learning techniques that require a significant amount of training data to learn useful representations from the data. Secondly, as our model learns features from the training data, it might not perform well when the trained model is applied to the data that have properties different from the training data such as data from different EEG channels. Our model has to be re-trained or fine-tuned before it can be applied to the data with different properties. Lastly, as our model utilizes bidirectional-LSTMs, the model has to wait until it has collected enough 30-s EEG epochs (depending on the sequence length of the EEG epochs used during the training process) before it can score these epochs. For instance, when the sequence length is set to 25, the model has to wait for 30*25 seconds (or 12.5 minutes) before it can identify sleep stages for these 25 EEG epochs.

VI. CONCLUSION AND FUTURE WORK

We proposed a deep learning model, named DeepSleepNet, for automatic sleep stage scoring based on raw single-channel EEG without utilizing any hand-engineered features. Our model utilizes CNNs to extract time-invariant features, and bidirectional-LSTMs to learn stage transition rules among sleep stages from EEG epochs. We also implemented the two-step training algorithm that pre-trains our model with the oversampled dataset to alleviate class-imbalance problems, and fine-tunes the model with the sequences of EEG epochs to encode the temporal information into the model. Our results showed that our model achieved a similar sleep stage scoring performance with the highest macro F1-score compared to the state-of-the-art hand-engineering methods. Our model analysis results also demonstrated that our model learned several features that are consistent with the AASM manual. As our model automatically learn features from raw EEG, we believe that DeepSleepNet is a better approach to realize a remote sleep monitoring compared to the hand-engineering ones.

In the future, we plan to improve our DeepSleepNet to be able to apply on the single-channel EEG such as the F4-EOG (Left) and Fp2-EOG (Left) collected from wearable devices.

ACKNOWLEDGMENT

The authors would like to thank Douglas McIlwraith and Axel Oehmichen from the Department of Computing, Imperial

College London who reviewed the contents of the paper, and provided support for running our cross-validation on the cluster of computing nodes.

REFERENCES

- [1] K. Wulff *et al.*, "Sleep and circadian rhythm disruption in psychiatric and neurodegenerative disease," *Nature Reviews Neuroscience*, vol. 11, no. 8, pp. 589–599, aug 2010.
- [2] J. Allan Hobson, "A manual of standardized terminology, techniques and scoring system for sleep stages of human subjects," *Electroencephalography and Clinical Neurophysiology*, vol. 26, no. 6, p. 644, jun 1969.
- [3] C. Iber *et al.*, *The AASM manual for the scoring of sleep and associated events*. American Academy of Sleep Medicine, 2007.
- [4] T. Lajnef *et al.*, "Learning machines and sleeping brains: Automatic sleep stage classification using decision-tree multi-class support vector machines," *Journal of Neuroscience Methods*, vol. 250, pp. 94–105, jul 2015.
- [5] S. Güne, K. Polat, and . Yosunkaya, "Efficient sleep stage recognition system based on EEG signal using k-means clustering based feature weighting," *Expert Systems with Applications*, vol. 37, no. 12, pp. 7922–7928, 2010.
- [6] O. Tsinalis, P. M. Matthews, and Y. Guo, "Automatic Sleep Stage Scoring Using Time-Frequency Analysis and Stacked Sparse Autoencoders," *Annals of Biomedical Engineering*, vol. 44, no. 5, pp. 1587–1597, may 2016.
- [7] L. Friawan *et al.*, "Automated sleep stage identification system based on time-frequency analysis of a single EEG channel and random forest classifier," *Computer Methods and Programs in Biomedicine*, vol. 108, no. 1, pp. 10–19, 2012.
- [8] S.-F. Liang *et al.*, "Automatic Stage Scoring of Single-Channel Sleep EEG by Using Multiscale Entropy and Autoregressive Models," *IEEE Transactions on Instrumentation and Measurement*, vol. 61, no. 6, pp. 1649–1657, jun 2012.
- [9] B. Koley and D. Dey, "An ensemble system for automatic sleep stage classification using single channel EEG signal," *Computers in Biology and Medicine*, vol. 42, no. 12, pp. 1186–1195, 2012.
- [10] M. Längkvist, L. Karlsson, and A. Loutfi, "Sleep Stage Classification Using Unsupervised Feature Learning," *Advances in Artificial Neural Systems*, vol. 2012, pp. 1–9, 2012.
- [11] O. Tsinalis *et al.*, "Automatic Sleep Stage Scoring with Single-Channel EEG Using Convolutional Neural Networks," *arXiv preprint arXiv:1610.01683*, 2016.
- [12] Y.-L. Hsu *et al.*, "Automatic sleep stage recurrent neural classifier using energy features of EEG signals," *Neurocomputing*, vol. 104, pp. 105–114, 2013.
- [13] H. Dong *et al.*, "Mixed Neural Network Approach for Temporal Sleep Stage Classification," *arXiv preprint arXiv:1610.06421*, 2016.
- [14] M. X. Cohen, *Analyzing Neural Time Series Data: Theory and Practice*. MIT Press, 2014.
- [15] S. Ioffe and C. Szegedy, "Batch Normalization: Accelerating Deep Network Training by Reducing Internal Covariate Shift," *arXiv preprint arXiv:1502.03167*, 2015.
- [16] K. He *et al.*, "Deep Residual Learning for Image Recognition," in *2016 IEEE Conference on Computer Vision and Pattern Recognition (CVPR)*. IEEE, jun 2016, pp. 770–778.
- [17] M. Schuster and K. Paliwal, "Bidirectional recurrent neural networks," *IEEE Transactions on Signal Processing*, vol. 45, no. 11, pp. 2673–2681, 1997.
- [18] S. Hochreiter and J. Schmidhuber, "Long Short-Term Memory," *Neural computation*, vol. 9, no. 8, pp. 1735–1780, 1997.
- [19] F. Gers and J. Schmidhuber, "Recurrent nets that time and count," in *Proceedings of the IEEE-INNS-ENNS International Joint Conference on Neural Networks. IJCNN 2000. Neural Computing: New Challenges and Perspectives for the New Millennium*, vol. 3, 2000, pp. 189–194 vol.3.
- [20] H. Sak, A. Senior, and F. Beaufays, "Long Short-Term Memory Based Recurrent Neural Network Architectures for Large Vocabulary Speech Recognition," *arXiv preprint arXiv:1402.1128*, 2014.
- [21] C. Szegedy *et al.*, "Rethinking the Inception Architecture for Computer Vision," *arXiv preprint arXiv:1512.00567*, 2015.
- [22] D. Kingma and J. Ba, "Adam: A method for stochastic optimization," *arXiv preprint arXiv:1412.6980*, 2014.
- [23] R. Pascanu, T. Mikolov, and Y. Bengio, "On the difficulty of training Recurrent Neural Networks," *arXiv preprint arXiv:1211.5063*, 2012.

- [24] N. Srivastava *et al.*, “Dropout : A Simple Way to Prevent Neural Networks from Overfitting,” *Journal of Machine Learning Research*, vol. 15, pp. 1929–1958, 2014.
- [25] W. Zaremba, I. Sutskever, and O. Vinyals, “Recurrent Neural Network Regularization,” *arXiv preprint arXiv:1409.2329*, 2014.
- [26] C. O'Reilly *et al.*, “Montreal Archive of Sleep Studies: an open-access resource for instrument benchmarking and exploratory research,” *Journal of Sleep Research*, vol. 23, no. 6, pp. 628–635, dec 2014.
- [27] T. D. Lagerlund, “Manipulating the magic of digital EEG: Montage reformatting and filtering,” *American Journal of Electroneurodiagnostic Technology*, vol. 40, no. 2, pp. 121–136, 2000.
- [28] M. Sokolova and G. Lapalme, “A systematic analysis of performance measures for classification tasks,” *Information Processing & Management*, vol. 45, no. 4, pp. 427–437, jul 2009.
- [29] M. Abadi *et al.*, “TensorFlow: Large-Scale Machine Learning on Heterogeneous Distributed Systems,” *arXiv preprint arXiv:1603.04467*, 2015.
- [30] A. Karpathy, J. Johnson, and L. Fei-Fei, “Visualizing and Understanding Recurrent Networks,” *arXiv preprint arXiv:1506.02078*, 2015.



Akara Supratak received the B.Sc. degree in Information and Communication Technology (International Program) from the Faculty of Information and Communication Technology, Mahidol University, Thailand in 2010, and the M.Sc degree in Computing (Software Engineering) from Imperial College London, United Kingdom in 2013.

He is currently a Ph.D. candidate at Data Science Institute, Department of Computing, Imperial College London. His research is in the area of bio-medical engineering, software engineering and machine learning. He has been focusing on applying deep learning to medical data, especially time series data.



Hao Dong received a first-class honours BEng degree in digital signal and image processing from Beijing Institute & Technology and University of Central Lancashire in 2011, and a Distinguish Master degree in Department of Computing (visual information processing group) from Imperial College London in 2012. He has held visiting position with Chinese Academy of Sciences. He also worked as a CTO at high-tech company in China.

He is now a Ph.D. candidate at Data Science Institute and Department of Computing, Imperial College London. His current research interests focus on deep learning, data acquisition and machine learning theory and applications in data driven research, especially in time series classification and automatic feature detection. He also concern about the field of advanced sensors. He is the recipient of Ph.D Scholarship and Outstanding Undergraduate Student Scholarship.



Chao Wu received his PhD degree from Zhejiang University, China. He is a Research Associate in Data Science Institute, Imperial College London. He has been working in Big data analysis, modelling and applications for more than five years. He has lead and participated a number of significant and large-scale data driven projects in healthcare and smart cities. He has published over 30 articles and papers.



Yike Guo received a first-class honours degree in Computing Science from Tsinghua University, China, in 1985 and received his Ph.D. in Computational Logic from Imperial College in 1993. He is currently a Professor of Computing Science in the Department of Computing at Imperial College London. His research is in the areas of large scale scientific data analysis, data mining algorithms and applications, parallel algorithms and cloud computing. He has been focusing on applying data analysis and data mining technologies to scientific data analysis in the fields of life science and healthcare and environment science since 1995 when he was the Technical Director of Imperial College Parallel Computing Center.